

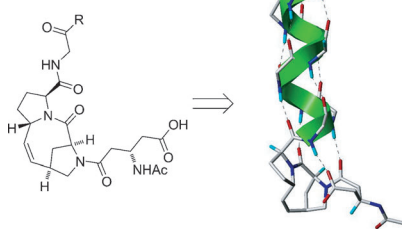
## Communications



### Peptide Structure

V. Hack, C. Reuter, R. Opitz, P. Schmieder,  
M. Beyermann, J.-M. Neudörfl,  
R. Kühne,\*  
H.-G. Schmalz\* ————— ■■■■-■■■■

Efficient  $\alpha$ -Helix Induction in a Linear  
Peptide Chain by N-Capping with  
a Bridged-tricyclic Diproline Analogue



**Secondary structure induction:** The synthetic tricyclic amino acid ProM-5, which is formally created by stereoselective introduction of a vinylidene bridge into a di-proline unit, acts as a powerful scaffold to nucleate  $\alpha$ -helix formation in a linear peptide chain. This might be exploited in the development of new proteomimetics for the modulation of protein interactions.

# Efficient $\alpha$ -Helix Induction in a Linear Peptide Chain by *N*-Capping with a Bridged-tricyclic Diproline Analogue\*\*

Verena Hack, Cédric Reuter, Robert Opitz, Peter Schmieder, Michael Beyermann, Jörg-Martin Neudörfl, Ronald Kühne,\* and Hans-Günther Schmalz\*

Dedicated to the Bayer company on the occasion of its 150th anniversary

The recognition of short amino acid sequences forming an  $\alpha$ -helical motif represents an important event in many protein–protein interactions (PPI), and misfolding of such motifs is often associated with diseases, including cancer and HIV.<sup>[1–3]</sup> Accordingly, the search for synthetic compounds stabilizing or mimicking the relevant secondary structure while properly presenting the key interaction residues to the recognizing protein surface constitutes a great challenge.<sup>[4]</sup> As the key structural properties defining the PPI of interest and their contribution to the free energy of the PPI are mostly not known, it would be attractive to identify these properties by using modified linear peptides with a defined (stabilized) secondary structure. However, conformational stabilization of a linear peptide is a complex task and several strategies were developed to address this problem. For instance, the helical propensity can be enhanced by means of a chemical linkage between the side chains of *i* and *i* + 4 residues.<sup>[5]</sup> Another concept uses unnatural oligomers such as peptoids<sup>[6]</sup> or  $\beta$ -peptides<sup>[7]</sup> adopting a helical conformation. Since mostly the surface built by the side chains of the residues *i*, *i* + 3 and/or *i* + 4, and *i* + 7 is important for  $\alpha$ -helix recognition, conformationally restricted scaffolds that orient functional residues in spatially defined positions (resembling the amino acid side chains) are promising mimics of short  $\alpha$ -helical peptides.<sup>[8]</sup> An elegant concept was introduced by Kemp and co-workers who devised conformationally restricted diproline templates positioned at the *N*-terminus of a peptide.<sup>[9]</sup> By pre-orienting the first four hydrogen bonds they achieved a bias in favor of the  $\alpha$ -helical secondary structure. However, the effects were not particularly pronounced owing to the biconformational behavior of the used scaffold in which the two proline units were bridged by a flexible thiomethylene

unit and only one of two conformers (equally populated in solution) exhibited the desired helix-inducing properties.<sup>[10]</sup>

Supported by molecular modeling, we envisioned that the scaffold ProM-5<sup>[11]</sup> (**1**), that is, a Pro-Pro analogue made rigid by means of an ethylidene bridge, should display better properties than the  $\alpha$ -helix-inducing *N*-cap presented by Kemp<sup>[9,10]</sup> because it should exhibit a more or less mono-conformational behavior (Figure 1).

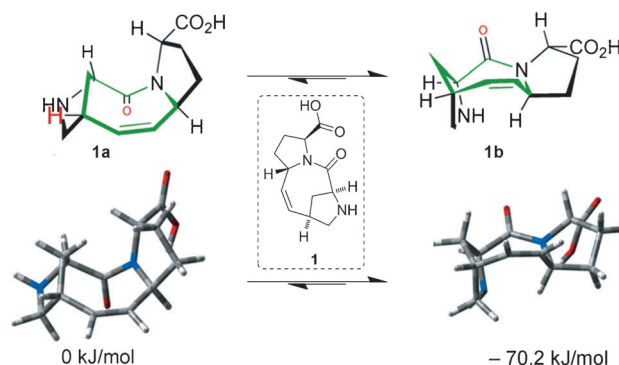
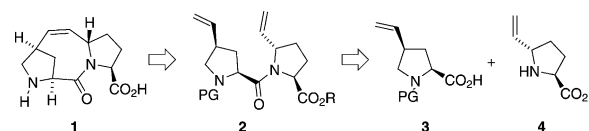


**Figure 1.** Structural representation of ProM-5 (**1**). The vinylidene bridge restricts the flexibility of the 8-membered ring strongly favoring the desired conformer **1b**. The energy difference between the conformers **1a** and **1b** was calculated based on DFT minimizations of both conformers in water (for details, see the Supporting Information).

According to our own modeling studies, and in agreement with the results of Kemp,<sup>[10]</sup> we expected the  $\alpha$ -helix-inducing capacity of the tricyclic scaffold **1** being strengthened through attachment of an Ac- $\beta$ HAsp residue to the *N*-terminus (Figure 2).

For the synthesis of the designed scaffold **1**, we devised the strategy sketched in Scheme 1. As a key feature, the bridged ring system is generated through Ru-catalyzed ring-closing metathesis from a dipeptidic precursor (**2**), which in turn would be derived from two protected vinylproline building blocks of type **3** and **4**.



**Scheme 1.** Retrosynthetic analysis of **1**.

[\*] Dr. V. Hack,<sup>[‡]</sup> Dr. C. Reuter,<sup>[‡]</sup> Dr. J.-M. Neudörfl, Prof. Dr. H.-G. Schmalz  
Universität zu Köln, Department für Chemie  
Greinstrasse 4, 50939 Köln (Germany)  
E-mail: schmalz@uni-koeln.de

Dr. R. Opitz,<sup>[‡]</sup> Dr. P. Schmieder, Dr. M. Beyermann, Dr. R. Kühne  
Leibniz-Institut für Molekulare Pharmakologie  
Robert-Rössle-Strasse 10, 13125 Berlin (Germany)  
E-mail: kuehne@fmp-berlin.de

[‡] These authors contributed equally to this work.

[\*\*] This work was supported by the Deutsche Forschungsgemeinschaft (DFG FOR 806) and Bayer HealthCare. We also thank Darius Kranz, Köln, for orienting energy calculations.

Supporting information for this article is available on the WWW under <http://dx.doi.org/10.1002/anie.201302014>.

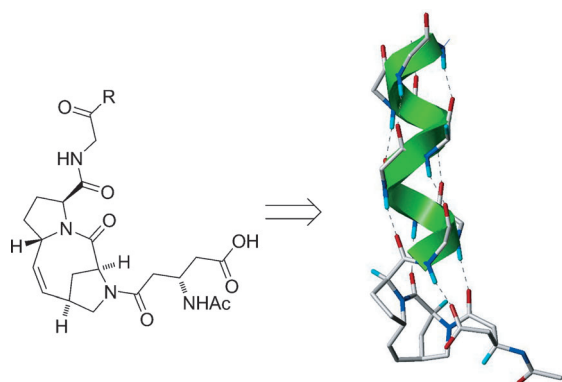
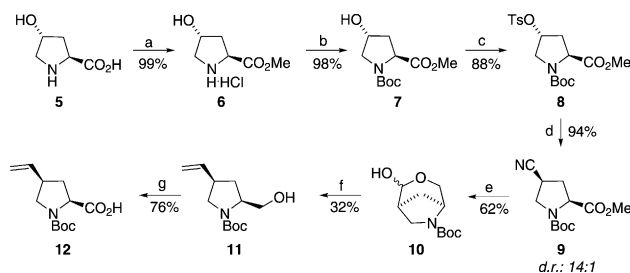


**Figure 2.** Model of an Ac- $\beta$ HAsp-[ProM-5]-capped  $\alpha$ -helical peptide. The four carbonyl oxygen atoms of the  $\beta$ HAsp-[ProM-5] take part in hydrogen bonds stabilizing the  $\alpha$ -helical secondary structure of the peptide.

As protecting groups, the combination of a *N*-Boc and a *tert*-butyl ester appeared to be most promising according to our previous experience.<sup>[12]</sup> The required building block of type **3**, that is, the (so far unknown) *N*-Boc-protected *cis*-4-vinylproline derivative **12**, was synthesized in a seven-step sequence (Scheme 2).



**Scheme 2.** Synthesis of the type **3** building block **12**: a)  $\text{SOCl}_2$ , MeOH, RT, 15 h, quant.; b)  $\text{Boc}_2\text{O}$ ,  $\text{NEt}_3$ , MeCN, RT, 15 h, 98%; c)  $\text{TsCl}$ ,  $\text{NEt}_3$ ,  $\text{CH}_2\text{Cl}_2$ , RT, 15 h, 88%; d)  $\text{NaCN}$ , DMSO,  $80^\circ\text{C}$ , 5 h, 94%; e)  $\text{DIBALH}$ ,  $\text{CH}_2\text{Cl}_2/n\text{Hex}$ ,  $-78^\circ\text{C}$  to RT, 7.5 h, 62%; f)  $\text{Ph}_3\text{PMeBr}$ , BuLi, THF/ $n\text{Hex}$ , RT, 2 h, 32%; g) TEMPO, BAIB, MeCN/ $\text{H}_2\text{O}$ , RT, 3 h, 76%. Boc = *tert*-butoxycarbonyl, DIBALH = diisobutylaluminum hydride, TEMPO = (2,2,6,6-tetramethylpiperidin-1-yl)oxyl, BAIB = bis-(acetoxy)iodobenzene, Ts = *para*-tolylsulfonyl.

Starting from commercially available (*S*)-*trans*-4-hydroxyproline (**5**), the double protected derivative **7** was prepared in high yield through methyl ester formation and Boc protection.<sup>[13]</sup> Activation of the OH group by tosylation<sup>[14]</sup> and treatment of the resulting intermediate **8** with NaCN in DMSO at  $80^\circ\text{C}$  then afforded the  $\text{S}_{\text{N}}2$  substitution product **9** with good diastereoselectivity (14:1).<sup>[15]</sup> Attempts to convert the nitrile to an aldehyde function through Raney-Ni-mediated hydrogenation<sup>[12]</sup> was associated with an epimerization at the 4-position, affording a 1:2 (*cis/trans*) mixture of diastereomeric aldehydes. In contrast, the reduction of **9** with DIBALH (3 equiv) proceeded without epimerization. The crude product (isolated in 62% yield and identified by NMR as the hemiacetal **10**) was directly converted by Wittig reaction to afford the vinyl prolinol derivative **11** as the

pure *cis* isomer after chromatography.<sup>[16]</sup> Finally, the re-oxidation of the side chain was achieved under mild conditions by TEMPO-mediated oxidation with bis-(acetoxy)iodobenzene (BAIB) in MeCN/water.<sup>[17]</sup> This way, the building block **12** was obtained (in 12% overall yield from **5**). Its relative configuration was secured by X-ray analysis (Figure 3).

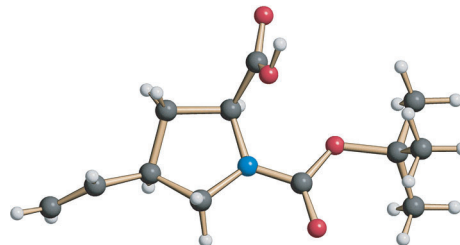
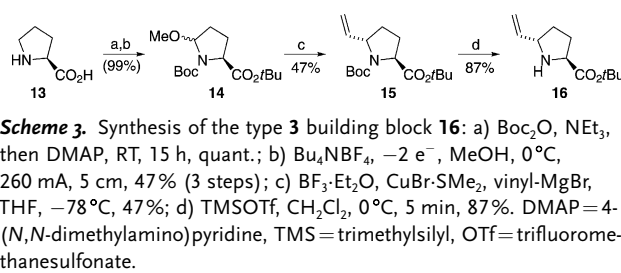


**Figure 3.** Structure of the *cis*-4-vinylproline **12** in the crystalline state. C gray, H white, O red, N blue.<sup>[38]</sup>

The second building block, that is, the *trans*-5-vinylproline derivative **16**, was synthesized as shown in Scheme 3. Exploiting our one-pot double-protection procedure,<sup>[18]</sup> (*S*)-proline (**13**) was first converted into the *N*-Boc-*tert*-butyles-

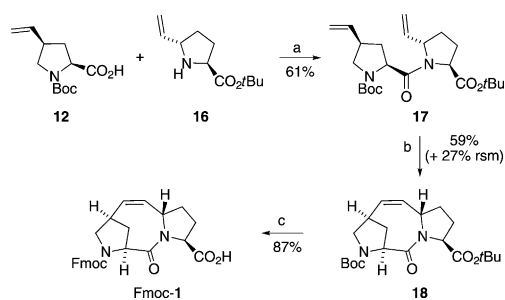


**Scheme 3.** Synthesis of the type **3** building block **16**: a)  $\text{Boc}_2\text{O}$ ,  $\text{NEt}_3$ , then DMAP, RT, 15 h, quant.; b)  $\text{Bu}_4\text{NBF}_4$ ,  $-2 e^-$ , MeOH,  $0^\circ\text{C}$ , 260 mA, 5 cm, 47% (3 steps); c)  $\text{BF}_3 \cdot \text{Et}_2\text{O}$ ,  $\text{CuBr} \cdot \text{SMe}_2$ , vinyl-MgBr, THF,  $-78^\circ\text{C}$ , 47%; d) TMSOTf,  $\text{CH}_2\text{Cl}_2$ ,  $0^\circ\text{C}$ , 5 min, 87%. DMAP = 4-(*N,N*-dimethylamino)pyridine, TMS = trimethylsilyl, OTf = trifluoromethanesulfonate.

ter, which was electrochemically oxidized<sup>[12b,19]</sup> to the methoxylated derivative **14**. The crude product (**14**) was then reacted with an excess of a vinyl MgBr-derived cuprate in the presence of  $\text{BF}_3 \cdot \text{Et}_2\text{O}$ , exactly following the procedure of Nagaïke et al.<sup>[20]</sup> to afford the pure *trans* isomer **15** (after chromatography) in 47% overall yield from **13** (3 steps). Selective cleavage of the *N*-Boc protecting group was smoothly achieved with TMSOTf ( $\text{CH}_2\text{Cl}_2$ ,  $0^\circ\text{C}$ , 5 min) to give the pure amine **16** after aqueous work-up. It should be mentioned that the configuration of **16** (obtained by a different route as a minor diastereomer) had been secured by X-ray crystal structure analysis in the course of our previous work.<sup>[12]</sup>

The connection of the two vinylproline building blocks **12** and **16** was then carried out using COMU<sup>[21]</sup> as a coupling reagent in the presence of Hünig's base to give **17** in 61% yield (Scheme 4). The comparable low yield of **17** reflects the steric bulkiness of the coupling partners.

An X-ray crystal structure analysis of the coupling product **17** (Figure 4) confirmed its expected configuration but also indicated an unfavorable pre-organization of the vinyl moieties with respect to cyclization. Nevertheless, the



**Scheme 4.** Synthesis of Fmoc-1: a) COMU, Et(*i*Pr)<sub>2</sub>N, MeCN, RT, 5 d, 61%; b) 30 mol% Grubbs II, toluene, Δ, 24 h, 59%; c) TFA, CH<sub>2</sub>Cl<sub>2</sub>, RT, 1 h, then Fmoc-Cl, NaHCO<sub>3</sub>, H<sub>2</sub>O/THF 2:1, RT, 15 h, 87%; COMU = 1-cyano-2-ethoxy-2-oxoethylideneaminoxy)dimethylaminomorpholinocarbenium hexafluorophosphate.

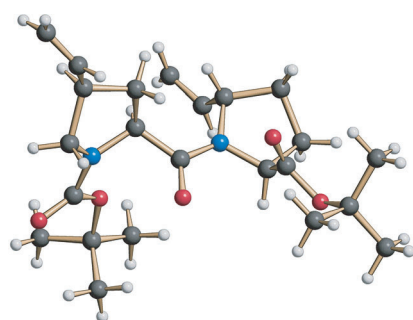


**Figure 4.** Structure of the dipeptide **17** in the crystalline state. C gray, H white, O red, N blue.<sup>[38]</sup>

projected ring-closing metathesis was successfully performed using 30 mol% of the Grubbs II catalyst. After chromatography, the desired bridged tricyclic product **18** was obtained in 59% yield along with 27% of recovered starting material (**17**). The cleavage of both protecting groups was accomplished by treatment of **18** with TFA in CH<sub>2</sub>Cl<sub>2</sub>. After solvent change to THF/water the final Fmoc-protection (Fmoc-Cl, NaHCO<sub>3</sub>) proceeded smoothly to give the projected target molecule (Fmoc-**1**) in 87% yield.

Using standard solid-phase Fmoc chemistry,<sup>[22]</sup> the scaffold **1** (that is, ProM-5) was then incorporated as a potential  $\alpha$ -helix-inducing unit into a peptide sequence derived from an  $\alpha$ -helical linker motif in peptide analogues of the peptide hormone urocortin.<sup>[23]</sup> Taking Ac- $\beta$ HAsp-Pro-Pro-Glu-Lys-Glu-Glu-Lys-Glu-Lys-Lys-Arg-Lys-Glu-NH<sub>2</sub> (P-1) as a reference, the corresponding peptide P-2, in which the Pro-Pro unit is replaced by ProM-5, was prepared (Table 1).

To investigate the  $\alpha$ -helix-inducing (nucleating) effect of the ProM-5 scaffold, we first looked at the CD spectra (20 mM potassium phosphate, pH 6.5, H<sub>2</sub>O, 2 °C) of peptides P-1 and P-2, respectively (Figure 5). For comparison purposes, we

**Table 1:** Sequences of the measured peptides.

Peptide	Sequence
P-1	Ac- $\beta$ HAsp- <b>Pro-Pro</b> -Glu-Lys-Glu-Glu-Lys-Glu-Lys-Lys-Arg-Lys-Glu-NH <sub>2</sub>
P-2	Ac- $\beta$ HAsp-[ <b>ProM-5</b> ]-Glu-Lys-Glu-Glu-Lys-Glu-Lys-Lys-Arg-Lys-Glu-NH <sub>2</sub>

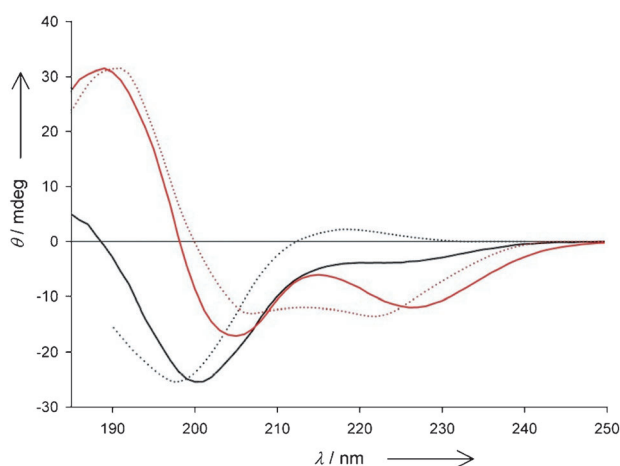


**Figure 5.** Far-UV CD spectra of peptides P-1 (black solid line) and P-2 (red solid line) in comparison to the spectra of random-coiled peptides (black dotted line) and 100%  $\alpha$ -helical poly-L-glutamic acid at low pH (red dotted line). The pairs of similar spectra were scaled to their maximum Cotton effects.

used the spectra of coiled peptides (poly-L-glutamic acid, poly-L-lysine, and others)<sup>[24]</sup> and of poly-L-glutamic acid in its  $\alpha$ -helical state.<sup>[25–28]</sup>

The CD spectrum of P-1 shows a negative Cotton effect at 201 nm indicating a mainly random-coiled (conformationally unordered) peptide chain, as also reflected by the similarity to the spectrum of an unordered peptide (negative Cotton effect near 195 nm). Much to our satisfaction, the CD spectrum of P-2, where the Pro-Pro unit is substituted by our  $\alpha$ -helix-inducing scaffold ProM-5, indicates a high degree of  $\alpha$ -helicity.<sup>[29]</sup> The observed Cotton effects (189 nm, 205 nm and 227 nm, respectively) and the zero-crossing (198 nm) differ only slightly from the ones reported for the ideal  $\alpha$ -helix of poly-L-glutamic acid at low pH (193 nm, 208 nm, 222 nm; zero-crossing at 200 nm).<sup>[24,26,27,30,31]</sup>

Further support for the  $\alpha$ -helical structure of P-2 was gained through NMR experiments. One-dimensional <sup>1</sup>H NMR spectra but also TOCSY<sup>[32]</sup> and <sup>1</sup>H-<sup>15</sup>N-SOFAST-HMQC<sup>[33]</sup> spectra were used to obtain secondary chemical shifts (Figure 6).

The secondary shifts of the H $\alpha$ , HN, and also N resonances<sup>[34]</sup> indicated an increase in helical content of P-2 as compared to the reference peptide P-1 (Figure 6). In the ROESY spectra,<sup>[35]</sup> we found an increased number of HN-HN cross peaks for P-2 as compared to P-1 (see the Supporting Information), suggesting that up to six residues of the peptide chain are involved in the proposed  $\alpha$ -helix. Even though no sequence-specific assignment was possible owing to signal overlap, the ROESY and TOCSY spectra showed a characteristic pattern, which allowed the conclusion that these residues are located prior to the only arginine in the sequence.

In our opinion, the results of the CD and NMR experiments clearly demonstrate a powerful  $\alpha$ -helix-inducing effect of the ProM-5 scaffold. However, the thermal folding

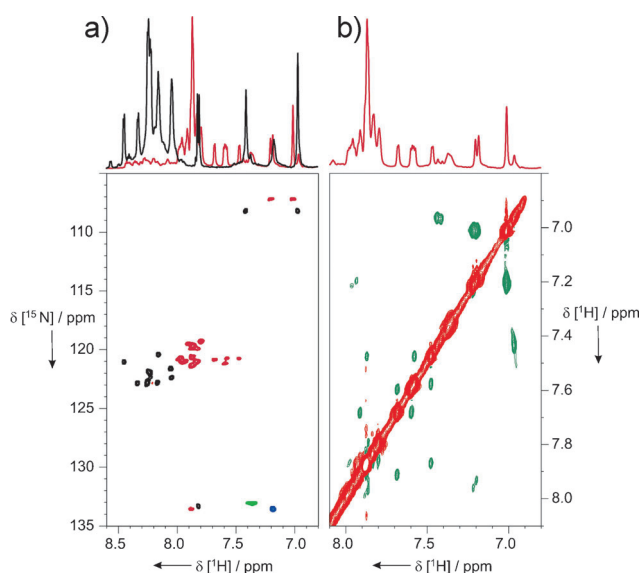


**Figure 6.** a)  $^1\text{H}$  NMR spectra of P-1 (black) and P-2 (red),  $^1\text{H}$ - $^{15}\text{N}$  SOFAST-HMQC of P-1 (black and green) and P-2 (red and blue); b) ROESY spectra of P-2 (cross-peaks in green).

stability of P-2 proved to be rather poor (as confirmed by CD-thermal shifts; see the Supporting Information), similar to the behavior of peptides containing Kemp's scaffold.<sup>[10]</sup> In the course of our study we were also able to show that in contrast to P-1 (which unfolds in a two-state process), the P-2 peptide unfolds in a more complex manner (for spectra, see the Supporting Information). This observation might be attributed to a progressing unfolding of the helix.

The relative  $\alpha$ -helical content of both peptides was determined through titration experiments monitored by CD spectroscopy (Figure 7). Such measurements are normally

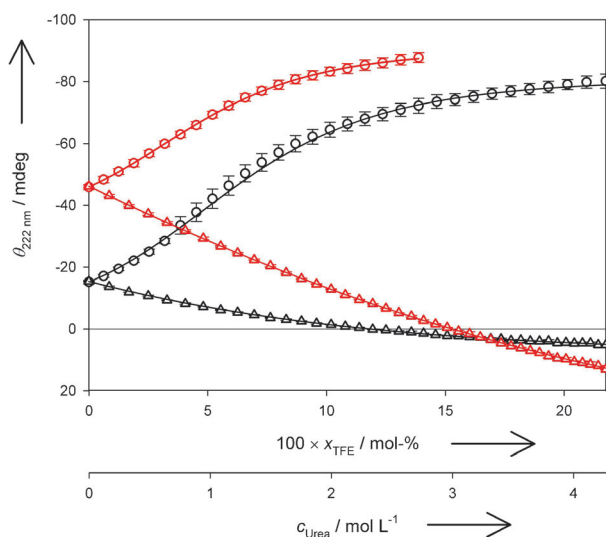


**Figure 7.** CD titration of P-1 (black) and P-2 (red) with TFE ( $\circ$ ) or urea ( $\Delta$ ) at 222 nm and 2°C. The CD signal was corrected for dilution effects and the background CD signal of the buffer (see the Supporting Information). Data were fitted to a two-state model to obtain the percentage of inducible  $\alpha$ -helical content (ca. 26% for P-1 and ca. 66% for P-2).

interpreted on the level of molar ellipticities.<sup>[27,36]</sup> However, the determination of the absolute peptide concentration by quantitative amino acid analysis or absorption measurements proved difficult in our case. We therefore applied a different approach based on the titration with trifluoroethanol (TFE), which induces  $\alpha$ -helical content in any peptide depending on the TFE concentration, the end-point of such a titration indicating 100%  $\alpha$ -helical content ( $\theta_{100\%}$ ). In contrast, titration with urea leads (especially for peptides containing glutamic acid or lysine)<sup>[36,37]</sup> to a complete unfolding of any secondary structure, the end-point corresponding to 0%  $\alpha$ -helical content ( $\theta_{0\%}$ ). Focusing on the CD signal at 222 nm (as a characteristic  $\alpha$ -helix maximum), these measurements allowed the percentage of the  $\alpha$ -helical content of both peptides to be calculated. After fitting the experimental data at 2°C with a simple two-state thermodynamic model (Figure 7) to obtain  $\theta_{100\%}$  and  $\theta_{0\%}$ , the percentage of inducible  $\alpha$ -helical content was calculated as 26% for P-1 and 66% for P-2. The relatively high  $\alpha$ -helical content of P-1 reflects the enhanced probability of the Glu-Lys-rich peptide to adopt an  $\alpha$ -helical secondary structure.<sup>[23]</sup>

In conclusion, we have demonstrated that the rigidified diproline mimetic ProM-5 (**1**), for which an efficient synthesis was elaborated, acts as a powerful  $\alpha$ -helix-inducing unit when embedded (as a *N*-cap) into a linear model peptide, as thoroughly analyzed by CD and NMR spectroscopy. In contrast to the rather flexible scaffold earlier introduced by Kemp,<sup>[10]</sup> our scaffold displays a mono-conformational behavior. Thus, ProM-5 is not only a promising module for the synthesis of  $\alpha$ -helical proteomimetics but also a novel  $\text{sp}^3$ -rich key building block (with stereodefined exit vectors) for the synthesis of meaningful screening libraries.

Received: March 10, 2013

Revised: April 11, 2013

Published online: ■■■■■, ■■■■■

**Keywords:** conformational analysis · molecular modeling · peptides and peptide mimics · protein–protein interactions · ring-closing metathesis

- [1] a) H. Jubb, A. P. Higuero, A. Winter, T. L. Blundell, *Trends Pharmacol. Sci.* **2012**, 33, 241–248; b) V. Azzarito, K. Long, N. S. Murphy, A. J. Wilson, *Nat. Chem.* **2013**, 5, 161–173; c) S. Asada, Y. Choi, M. Uesugi, *J. Am. Chem. Soc.* **2003**, 125, 4992–4993.
- [2] a) A. Shaginian, L. R. Whitby, S. Hong, I. Hwang, B. Farooqi, M. Searcey, J. Chen, P. K. Vogt, D. L. Boger, *J. Am. Chem. Soc.* **2009**, 131, 5564–5572; b) L. R. Whitby, K. E. Boyle, L. Cai, X. Yu, M. Gochin, D. L. Boger, *Bioorg. Med. Chem. Lett.* **2012**, 22, 2861–2865; c) L. R. Whitby, D. L. Boger, *Acc. Chem. Res.* **2012**, 45, 1698–1709.
- [3] a) J. A. Hebda, I. Saraogi, M. Magzoub, A. D. Hamilton, A. D. Miranker, *Chem. Biol.* **2009**, 16, 943–950; b) G. C. Cummings, A. D. Hamilton, *Curr. Opin. Chem. Biol.* **2010**, 14, 341–346.
- [4] a) J. A. Wells, C. L. McClendon, *Nature* **2007**, 450, 1001–1009; b) L. Jochim, P. S. Arora, *ACS Chem. Biol.* **2010**, 5, 919–923.
- [5] Y. Che, B. R. Brooks, G. R. Marshall, *Biopolymers* **2007**, 86, 288–297.
- [6] R. J. Simon, R. S. Kania, R. N. Zuckermann, V. D. Huebner, D. A. Jewell, S. Banville, S. Ng, L. Wang, S. Rosenberg, C. K. Marlowe, *Proc. Natl. Acad. Sci. USA* **1992**, 89, 9367–9371.

- [7] T. Kimmerlin, R. Sebesta, A. M. Campo, A. K. Beck, D. Seebach, *Tetrahedron* **2004**, *60*, 7455–7506.
- [8] a) H. Yin, A. D. Hamilton, *Angew. Chem.* **2005**, *117*, 4200–4235; *Angew. Chem. Int. Ed.* **2005**, *44*, 4130–4163; b) H. Yin, G. I. Lee, K. A. Sedey, J. M. Rodriguez, H. G. Wang, S. M. Sebti, A. D. Hamilton, *J. Am. Chem. Soc.* **2005**, *127*, 5463–5468; see also: c) C. P. Gomes, A. Metz, J. W. Bats, H. Gohlke, M. W. Göbel, *Eur. J. Org. Chem.* **2012**, 3270–3277; and references cited therein.
- [9] a) D. S. Kemp, J. G. Boyd, C. C. Muendel, *Nature* **1991**, *352*, 451–454; see also: b) D. S. Kemp, J. G. Boyd, C. C. Muendel, *J. Am. Chem. Soc.* **2006**, *128*, 7917–7928.
- [10] B. Heitmann, G. E. Job, R. J. Kennedy, S. M. Walker, D. S. Kemp, *J. Am. Chem. Soc.* **2005**, *127*, 1690–1704.
- [11] We use the term ProM-X to specify certain proline-derived modules for proteomimetic synthesis developed in our laboratories.
- [12] a) J. Zaminer, C. Brockmann, P. Huy, R. Opitz, C. Reuter, M. Beyermann, C. Freund, M. Müller, H. Oschkinat, R. Kühne, H.-G. Schmalz, *Angew. Chem.* **2010**, *122*, 7265–7269; b) C. Reuter, P. Huy, J.-M. Neudörfl, R. Kühne, H.-G. Schmalz, *Chem. Eur. J.* **2011**, *17*, 12037–12044.
- [13] a) K. S. Lee, J. H. Lim, Y. K. Kang, K. H. Yoo, D. C. Kim, K. J. Shin, D. J. Kim, *Eur. J. Med. Chem.* **2006**, *41*, 495–503; b) T. Honda, R. Takahashi, H. Namiki, *J. Org. Chem.* **2005**, *70*, 499–504; c) K. K. Schumacher, J. Jiang, M. M. Joulie, *Tetrahedron: Asymmetry* **1998**, *9*, 47–54.
- [14] a) K. Hamacher, *J. Labelled Compd. Radiopharm.* **1999**, *42*, 1135–1144; b) R. Caputo, M. Dellagrecia, I. De Paola, L. Longobardo, D. Mastroianni, *Amino Acids* **2010**, *38*, 305–310.
- [15] R. J. Bridges, M. S. Stanley, M. W. Anderson, C. W. Cotman, A. R. Chamberlin, *J. Med. Chem.* **1991**, *34*, 717–725.
- [16] S. Scapecchi, R. Matucci, C. Bellucci, M. Buccioni, S. Dei, L. Guandalini, C. Martelli, D. Manetti, E. Martini, G. Marucci, M. Nesi, M. N. Romanelli, E. Teodori, F. Gualtieri, *J. Med. Chem.* **2006**, *49*, 1925–1931.
- [17] J. B. Epp, T. S. Widlanski, *J. Org. Chem.* **1999**, *64*, 293–295.
- [18] P. Huy, H.-G. Schmalz, *Synthesis* **2011**, 954–960.
- [19] K. F. McClure, P. Renold, D. S. Kemp, *J. Org. Chem.* **1995**, *60*, 454–457.
- [20] F. Nagaike, Y. Onuma, C. Kanazawa, H. Hojo, A. Ueki, Y. Nakahara, Y. Nakahara, *Org. Lett.* **2006**, *8*, 4465–4468.
- [21] A. El-Faham, R. Subirós Funosas, R. Prohens, F. Albericio, *Chem. Eur. J.* **2009**, *15*, 9404–9416.
- [22] I. Coin, M. Beyermann, M. Bienert, *Nat. Protoc.* **2007**, *2*, 3247–3256.
- [23] M. Beyermann, S. Rothemund, N. Heinrich, K. Fechner, J. Furkert, M. Dathe, R. Winter, E. Krause, M. Bienert, *J. Biol. Chem.* **2000**, *275*, 5702–5709.
- [24] J. Reed, T. A. Reed, *Anal. Biochem.* **1997**, *254*, 36–40.
- [25] N. Sreerama, S. Y. Venyaminov, R. Woody, *Anal. Biochem.* **2000**, *287*, 243–251.
- [26] G. Böhm, R. Muhr, R. Jaenicke, *Protein Eng.* **1992**, *5*, 191–191.
- [27] N. J. Greenfield, *Nat. Protoc.* **2007**, *1*, 2876–2890.
- [28] M. L. Tiffany, S. Krimm, *Biopolymers* **1969**, *8*, 347–359.
- [29] As the ratio of the two minima  $\Theta_{226}/\Theta_{205}=0.70$  of P-2 is not distinctly lower than unity (and unordered content will contribute to the observed CD spectrum), we can exclude a significant amount of 3(10) helix content for P-2. Also, the pronounced Cotton effect at about 190 nm reflects an  $\alpha$ -helix, rather than a 3(10) helix; compare: a) C. Toniolo, A. Polese, F. Formaggio, M. Crisma, J. Kamphuis, *J. Am. Chem. Soc.* **1996**, *118*, 2744–2745; b) Z. Biron, S. Khare, A. O. Samson, Y. Hayek, F. Naider, J. Anglister, *Biochemistry* **2002**, *41*, 12687–12696.
- [30] L. A. Compton, W. C. Johnson, *Anal. Biochem.* **1986**, *155*, 155–167.
- [31] G. Holzwarth, P. Doty, *J. Am. Chem. Soc.* **1965**, *87*, 218–228.
- [32] a) J. Cavanagh, M. Rance, *J. Magn. Reson.* **1992**, *96*, 670–678; b) A. Bax, D. G. Davis, *J. Magn. Reson.* **1985**, *65*, 355–360.
- [33] P. Schanda, E. Kupce, B. Brutscher, *J. Biomol. NMR* **2005**, *33*, 199–211.
- [34] D. S. Wishart, B. D. Skyes, *Methods Enzymol.* **1994**, *239*, 363–392.
- [35] a) A. A. Bothner-By, R. L. Stephens, J. Lee, C. D. Warren, R. W. Jeanloz, *J. Am. Chem. Soc.* **1984**, *106*, 811–813; b) H. Kessler, C. Griesinger, R. Kerssebaum, K. Wagner, R. R. Ernst, *J. Am. Chem. Soc.* **1987**, *109*, 607–609.
- [36] B. Forood, E. J. Feliciano, K. P. Nambiar, *Proc. Natl. Acad. Sci. USA* **1993**, *90*, 838–842.
- [37] M. L. Tiffany, S. Krimm, *Biopolymers* **1973**, *12*, 575–587.
- [38] CCDC 932373 (12) and CCDC 932374 (17) contain the supplementary crystallographic data for this paper. These data can be obtained free of charge from The Cambridge Crystallographic Data Centre via [www.ccdc.cam.ac.uk/data\\_request/cif](http://www.ccdc.cam.ac.uk/data_request/cif).